Journal of Cleaner Production 165 (2017) 273–280

Contents lists available at ScienceDirect

Journal of Cleaner Production

journal homepage: www.elsevier.com/locate/jclepro

Integrating photovoltaic solar energy and a battery energy storage system to operate a semi-autogenous grinding mill

G. Pamparana [a, b], W. Kracht [a, b, *], J. Haas [c, d], G. Díaz-Ferrán [c, e], R. Palma-Behnke [c, f], R. Román [c, e]

[a] Department of Mining Engineering, Universidad de Chile, Chile
[b] Advanced Mining Technology Center, AMTC, Universidad de Chile, Chile
[c] Energy Center, Universidad de Chile, Chile
[d] Department of Stochastic Simulation and Safety Research for Hydrosystems (IWS/SC Simtech), University of Stuttgart, Germany
[e] Department of Mechanical Engineering, Universidad de Chile, Chile
[f] Department of Electrical Engineering, Universidad de Chile, Chile

ARTICLE INFO

Article history:
Received 20 October 2016
Received in revised form
21 June 2017
Accepted 15 July 2017
Available online 17 July 2017

Keywords:
Sustainable mining
Solar energy
Battery energy storage system
Semi-autogenous grinding mill
Demand side management

ABSTRACT

The mining sector in Chile is facing a steady increase of energy consumption, which is mainly explained by the lower grades, the increase in rock hardness, and deeper mines. Although much of the mining activity in Chile is located in the Atacama Desert, where the solar radiation is high, the integration of solar energy in mining remains elusive. This work explores, through simulation, the use of a solar photovoltaic energy system (PV) and a battery energy storage system (BESS), combined with energy from the grid, to operate a semi-autogenous grinding mill (SAG). For this, a novel mixed-integer linear programming model was developed to optimize the operational costs of the joint SAG-PV-BESS operation, after which the best sizes of PV and BESS components are found through scenario inspection. Further, the implementation of a demand side management (DSM) option is considered by a proper sequencing of the SAG feed to make a more efficient use of the solar energy. The results show an interdependent behavior of the SAG-PV-BESS system and a strong influence of DSM. The use of both PV and BESS allows reducing the contracted power for the SAG, without incurring into overconsumption penalties. If DSM is implemented, the system allocates the higher consumption, associated to harder ore, during daytime to use the available PV energy. Overall, the combined effect of PV and BESS operation of SAG mills allows reducing the energy-associated operational costs. This effect is exacerbated when DSM is implemented.

1. Introduction

The Chilean copper mining sector is facing several challenges. From an energy perspective, a steady increase of energy consumption is observed, explained by the lower mineral grades, increase in rock hardness and deeper mines (Harmsen et al., 2013; Cochilco, 2013). Additionally, the country's CO_2 targets motivate the sector to transit to a cleaner production (McLellan et al., 2012). Coincidentally, much of the copper mining extraction occurs in the Atacama Desert, where the solar radiation level is high, and the levelized costs of energy (i.e., the average energy costs of a given energy source, considering investment and operational costs) of photovoltaic (PV) power plants have become competitive even in absence of subsidies (Fuentealba et al., 2015), thus, emerging as a valuable choice for mining activities.

In Chile, comminution is responsible —in average— for almost 50% of the electrical energy consumption of the entire copper mining process (Cochilco, 2013), being the largest greenhouse gas emitter in the copper concentrate production (Norgate and Haque, 2010). Semi-autogenous grinding mills (SAG) are energy intensive, and operate with a variable power profile, mainly explained by the variable feed rate and ore hardness. These are difficult to forecast (Mosher and Bigg, 2001; Morrell, 2004), and have a strong impact on the power scheduling and the involved energy costs. In fact, mining companies in Chile pay for consumed energy (in $/MWh) and contracted power (in $/MW). In case the contracted power is exceeded, a fine in terms of that excess (difference between the maximum power consumption and the contracted power) is applied.

* Corresponding author. Advanced Mining Technology Center, Universidad de Chile, Chile.
E-mail address: wkracht@uchile.cl (W. Kracht).

http://dx.doi.org/10.1016/j.jclepro.2017.07.110
0959-6526/

The aforementioned variability and uncertainty might be exacerbated when a PV system is added to the copper production. In other industries, battery energy storage systems (BESS) are a frequent solution to these issues. Nowadays, there are many different BESS technologies, each with characteristic power and energy capacities, reaction times, lifetimes and costs (Beaudin et al., 2010). Hence, their type and size vary strongly with the application. An updated database of worldwide battery energy storage systems is provided by the U.S. Department of Energy (US Department of Energy, 2016). To mention a few, the "Gills Onions" BESS (Vanadium Redox flow, 0.6 MW, 6 h of storage) in the U.S., smoothens the energy demand of a biogas production; Tehachapi Wind Energy Storage Project (Li-ion, 8 MW, 4 h of storage), also in the U.S., improves the grid performance (voltage and frequency control, congestion management, reliability, etc.). Similarly, Los Andes Substation BESS (Li-ion, 12 MW, 0.3 h of storage) in Chile supports the stability of the electric grid; and Ford used a BESS (Lead acid, 0.8 MW, 2.6 h of storage) for integrating photovoltaic power into their car manufacturing.

Finding the optimal size and type of BESS in the context of integration of variable renewable energy systems has been object of research since the 90's. Initially, the approaches were based on a simple energy balance (Schoenung and Burns, 1996; Protogeropoulos et al., 1997). In time, the models have gained more operational details, including their energy and power capacity, and energy balance equation with up to hourly resolution for a whole planning year (Steinke et al., 2013; Schill, 2014; Zerrahn and Schill, 2015). Other operational phenomena, such as self-discharge, variable efficiency and temperature requirements, are often neglected. Also, aging (reduced lifetime of a BESS as a consequence of responding to frequent fluctuations) is rarely captured in expansion planning of storage systems, with the exception of only a few studies (Hajipour et al., 2015; Yao et al., 2009). A comprehensive review about the challenges for energy storage expansion decisions can be found in (Haas et al., 2017). In the planning of mining operations, considering PV systems and BESS is not well understood but desirable for improved reliability, good practices, cost savings and emission reduction. (Levesque et al., 2014).

The main cause of the SAG energy fluctuation is the variability of the rock hardness (Workman and Eloranta, 2003). In contrast to a conventional mining operation, where the power systems assumes the responsibility of buffering these fluctuations, a SAG-PV-BESS system would benefit from a more flexible load. For example, concentrating load during daytime would reduce the investment costs of BESS. This can be achieved by managing the SAG's feed with the aid of stockpiles, in such a way that hard ore is processed during the day and soft ore during the night (henceforth referred to as Demand Side Management, DSM). The implementation of DSM brings new challenges to the design and operation of mines and concentrators, and may have an impact on the integration of renewable energies in the copper mining process. However, the impact of implementing DSM has not been explored in the literature.

This work aims to explore the synergies that can occur through the implementation of a combined SAG-PV-BESS system. Using an optimization based simulation, we will explore how the variability of the SAG mill power consumption can be reduced and stabilized by using a PV-BESS system. This should lead to a cost reduction when considering the total costs (investment, operation and replacement). The DSM is also modeled, showing the impact it has on the combined system and its integration potential.

This paper makes the following contributions: i) it develops a novel mixed-integer linear programming model to optimize the operational costs of a PV-BESS-SAG system and determines through scenario inspection, the best sizes of the PV-BESS system components (including the BESS cycling costs); ii) it models and assesses the impact of a novel DSM option when planning such a combined system based on the sequencing of the SAG feed; and iii) it proposes a heuristic to reduce the resulting computing times.

2. Methods

The working hypothesis of this paper is that BESS can provide multiple services in the context of PV integration into a SAG mill operation, such as energy balance and planning power contracts. For this, a novel optimization model is proposed that minimizes the operational costs of the system composed by SAG mills, PV and BESS (SAG-PV-BESS), including costs for battery replacement due to cycling. This corresponds to a mixed-integer linear programming model, which was implemented using the function *intlinprog* (MATLAB Documentation, 2014), available in the optimization toolbox in MATLAB®. This solver uses the following algorithms: i) linear programming preprocessing and mixed integer programming preprocessing; ii) attempt for Cut Generation; iii) Branch and Bound to search through branches of the candidate solution tree (formed by the integer variables); iv) Interior-Point algorithm to solve the resulting linear program of each branch.

Optimizing the size of power plants together with their operation is computationally expensive, which is why simplifications have to be made. In the literature it can be seen that when focus is put on the operational detail, hybrid formulations are a frequent choice. These, rather than formulating a global optimization for investment and operation of the system, minimize only the operational costs and find, via scenario inspection, alternative system sizes (Suazo-Martínez et al., 2014). This work follows that logic; it uses optimization to find operational costs and scenario inspection to find the best sizes of the PV and BESS systems. Further operational flexibility can be achieved by managing the feed to the SAG mills, i.e., adapting the power consumption to the availability of the PV system and BESS by considering the tonnage and rock hardness during the operation, as both have a direct influence on the mill's load. For this, a sub-model was developed to simulate alternative sequencing of the ore being fed to the plant, which constitutes a DSM option that could allow consequent cost savings and a deeper solar energy penetration.

In summary, two model approaches are proposed and tested in a case study with sensitivity analysis: Model I without DSM, and Model II with DSM. In both models, the decision variables are the BESS and PV operation, and the grid imported and exported energy. For Model II, an additional decision variable is they way DSM is fulfilled.

2.1. Nomenclature

The nomenclature used in shown in Tables 1 and 2 for the decision variables and parameters, respectively. The convention used to describe them is to use capital letters for parameters and small letters for variables, where bolded letters are matrices.

2.2. Optimization model

The model considers a SAG mill operation connected to the grid, a PV power plant and a BESS (Fig. 1). Missing and excess energy can be bought from and sold to the grid. The model minimizes the total operational costs of running the SAG taking into account the cost of penalties when exceeding the contracted power, cost of imported (purchased) energy, income of exported (sold) energy, and cost of the BESS in terms of cycling.

Sizing the PV and BESS, as well as the power capacity contracts,

Table 1
Decision variables.

Variable	Description	Unit
p_t^{SAG}	Rearranged load of SAG mills at time t	MW
p_t^{imp}	Power imported from the grid at time t	MW
p_t^{exp}	Power exported to the grid at time t	MW
p_t^{s}	Power generated by the photovoltaic system at time t	MW
p_t^{bdis}	Power discharged from the batteries at time t	MW
p_t^{bch}	Power charged to the batteries at time t	MW
soc_t	State of charge of the batteries at time t (fraction)	–
p_{max}^{imp}	Maximum power bought from the grid during T	MW
$\boldsymbol{a_{it}}$	$(i \times t)$ binary variable matrix used for rearranging SAG power consumption	–
b_t^{dis}	Binary variable, 1 when BESS is discharging at time t	–
t	Index for time steps from 1 to T ($t \cdot dt$ = actual time in hours)	–
i	Index from 1 to T	–

Table 2
Parameters.

Parameter	Description	Unit
T	Number of time steps	–
dt	Length of time step	Hours
C_{con}	Contracted power cost	US$/MW
$C_{penalty}$	Penalty for over consumption	US$/MW/year
P_t^{SAG}	Original load of SAG mills at time t	MW
E_{max}^{bat}	Energy capacity of batteries	MWh
P_{max}^{bat}	Max. power capacity of batteries, limited by inverter	MW
C_{exp}	Selling price of energy	US$/MWh
C_{imp}	Purchase price of energy	US$/MWh
P_{con}	Contracted power capacity	MW
SOC_{min}	Minimum state of charge (fraction of E_{max}^{bat})	–
SOC_{max}	Maximum state of charge (fraction of E_{max}^{bat})	–
Inv_{bat}	BESS investment cost	US$/MWh
N_{max}^{cycles}	BESS life time measured in cycles	–
η_{bch}	Charging efficiency of BESS	–
η_{bdis}	Discharging efficiency of BESS	–

is not considered endogenously in the optimization. Instead, for these parameters, scenario inspection is used in order to find cost optimal dimensions. The objective function and the constraints of the optimization model are explained below.

2.3. Objective function

The objective function minimizes the total energy operational cost (OC) of the SAG mill (Equation (1)), including the battery replacement cost due to cycling, but excluding other costs such as grinding media.

$$\begin{aligned} min\, OC = {} & P_{con} \cdot C_{con} + \left(p_{max}^{imp} - P_{con}\right) \cdot C_{penalty} - \sum_{t=1}^{T} p_t^{exp} \cdot C_{exp} \cdot dt \\ & + \sum_{t=1}^{T} p_t^{imp} \cdot C_{imp} \cdot dt \\ & + \sum_{t=1}^{T} \left(\frac{\left(p_t^{bdis} + p_t^{bch}\right) \cdot dt}{2E_{max}^{bat} \cdot (SOC_{max} - SOC_{min})} \frac{Inv_{bat} \cdot E_{max}^{bat}}{N_{max}^{cycles}} \right) \end{aligned} \quad (1)$$

The first term is the contracted power capacity cost. Both P_{con} and C_{con} are inputs to the problem. The second term is the penalty cost, given by the difference between the maximum imported power (optimization variable) and the contracted capacity. The third and fourth terms are the total cost of exported and imported energy, respectively. The last term is the cycling cost of the BESS, which is expressed as a cost per cycle (BESS investment/replacement cost divided by its nominal number of cycles). The first division corresponds to the fraction of energy used (charge and discharge) from the total energy capacity of the BESS (considering maximum and minimum state of charge SOC). The second division expresses the cost per cycle of the BESS. One cycle equals to fully charging and discharging the BESS, up to a given depth of discharge. Until the end of the BESS' lifetime, its other parameters (energy and power capacity, and efficiency) are considered constants.

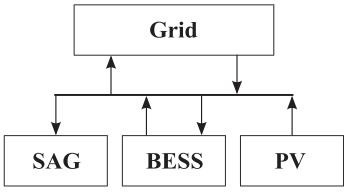

Fig. 1. Schematic of the system.

2.4. Constraints

2.4.1. System energy balance constraints

$$\left(p_t^{imp} - p_t^{exp} + p_t^{s} - p_t^{bch} + p_t^{bdis} - p_t^{SAG}\right) \cdot dt = 0 \quad \forall\ t \quad (2)$$

$$p_t^{SAG} = \sum_{i=1}^{T} \boldsymbol{a_{it}} \cdot P_i^{SAG} \quad \forall\ t \tag{3}$$

$$\sum_{i=1}^{T} \boldsymbol{a_{it}} = 1 \quad \forall\ t, \sum_{t=1}^{T} \boldsymbol{a_{it}} = 1 \quad \forall\ i \tag{4}$$

Equation (2) shows the energy balance between the imported and exported energy (p_t^{imp} and p_t^{exp}), the solar energy generated by the PV plant (p_t^s), the energy involved in the BESS charging and discharging stages (p_t^{bch} and p_t^{bdis}), and the energy consumed by the SAG mill(s) (p_t^{SAG}).

Equations (3) and (4) allow the operator re-arranging the ore feed, which translates into a manageable power demand. In this simulation it is assumed that the operator can freely sequence the ore of the whole time horizon (one day). This keeps the overall energy demand constant, but provides an additional degree of freedom for cost reduction. This practice is limited by the size of the stockpiles, which is not considered in the modeling. For modeling this, variable $\boldsymbol{a_{it}}$ is used (Equation (4)). In Model I (without DSM), no change in demand occurs and $\boldsymbol{a_{it}}$ form an identity matrix. This means that p_i^{SAG} behaves as a parameter in this model. In Model II (with DSM), it corresponds to a permutation of the identity matrix that allows rearranging the original load (P_i^{SAG}) while assuring that each element is only used once (sum of each row and column equals to one). The product $\boldsymbol{a_{it}} \cdot P_i^{SAG}$ results in a new sequence of power consumption for the SAG mill due to DSM.

2.4.2. Maximum imported power constraint

$$p_t^{imp} - p_{max}^{imp} \leq 0 \quad \forall\ t \tag{5}$$

$$P_{con} \leq p_{max}^{imp} \tag{6}$$

The maximum imported power variable, p_{max}^{imp}, is used to calculate the penalty of overconsumption for a given contracted power value. Equation (5) saves the value of maximum imported power.

Equation (6) defines p_{max}^{imp} as P_{con} if overconsumption does not occur, implying that the penalty in Equation (1) is zero. Conversely, if overconsumption does happen, the imported power (p_t^{imp}) is higher than the contracted power (P_{con}), and the penalty in the objective function becomes positive.

2.4.3. Energy balance in the BESS

$$soc_{t+1} \cdot E_{max}^{bat} = soc_t \cdot E_{max}^{bat} + p_t^{bch} \cdot \eta_{bch} \cdot dt - p_t^{bdis} \cdot \frac{1}{\eta_{bdis}} \cdot dt \quad \forall\ t \tag{7}$$

$$SOC_{min} \leq soc_t \leq SOC_{max} \quad \forall\ t \tag{8}$$

In Equation (7), the energy balance of the BESS at $t+1$ ($soc_{t+1} \cdot E_{max}^{bat}$), equals to the energy stored at the previous period t $\left(soc_t \cdot E_{max}^{bat}\right)$, plus the energy charged ($p_t^{bch} \cdot \eta_{bch} \cdot dt$), minus the energy discharged ($p_t^{bdis} \cdot \frac{1}{\eta_{bdis}} \cdot dt$), considering conversion losses given by their corresponding efficiencies. Equation (8) defines a minimum (SOC_{min}) and maximum (SOC_{max}) value for the state of charge of the batteries (soc_t).

2.4.4. Battery charge or discharge status constraint

$$p_t^{bdis} - b_t^{dis} \cdot P_{max}^{bat} \leq 0 \quad \forall\ t \tag{9}$$

$$p_t^{bch} - \left(1 - b_t^{dis}\right) \cdot P_{max}^{bat} \leq 0 \quad \forall\ t \tag{10}$$

Equation (9) ensures that the BESS discharging power (p_t^{bdis}) is always limited by its maximum capacity (P_{max}^{bat}). The binary variable b_t^{dis} is used to ensure that the BESS only discharges when turned on, while Equation (10) is analogous for BESS charging power (p_t^{bch}). The expression $(1 - b_t^{dis})$ is used to avoid that BESS charges and discharges simultaneously.

2.5. Case study

2.5.1. Case definition and input data

The models are applied to a theoretical case study. Four cases, in addition to the base case, are studied using the models proposed earlier. Table 3 describes each case.

The variables subjected to sensitivity are the size of PV plant in C1, the contracted capacity in C2, the BESS energy capacity in C3, and the BESS power capacity in C4.

As what refers to the inputs, a SAG mill power consumption data and actual PV generation curves located on the Atacama Desert in Chile are used. A data set with a 15-min time resolution was used for a simulation period of one day. The SAG data corresponds to the operation of three mills over six months, from which a typical day was selected through fuzzy c-means clustering. The total production for this typical day was 192,000 tons for the three SAG mills, with a maximum and minimum SAG mill power consumption of 42.17 MW and 40.77 MW, respectively. The average consumption for the day was 41.58 MW.

The price of selling and purchasing energy is 70 US$/MWh and 85 US$/MWh, respectively, whereas the price of contracted power (converted to the daily time horizon) is 40 US$/MW and overpower consumption is 15 kUS$/MW. These values are highly variable in time and are case-specific.

The model is general enough to consider any type of batteries. In the case study the storage system consists of flooded lead acid batteries with a fixed energy-to-power ratio of 5 MWh per MW for the BC, C1, and C2, and with a variable ratio for C3 and C4. A lifespan of 1500 cycles at 70% of depth of discharge (Suberu et al., 2014) is considered. The initial and final state of charge was set to 50%, and the maximum and minimum state of charge to 90% and 20%, respectively. The BESS efficiency for both charging and discharging was assumed to be 95%.

The annuities of the investment costs are calculated considering a lifetime of 30-years and a 10% discount rate. The considered investment costs are 110 kUS$/MWh for the BESS and 1770 kUS$/MW for the PV system (Chung et al., 2015). The resulting costs are translated into daily values.

The simulations were run in a computer with a 3.5 GHz octa-core processor and 16 GB of RAM using the optimization toolbox from MATLAB®. Model I has about 960 variables of which 96 are binaries and takes in average 0.5 s to run, while Model II has 10,180 variables of which 9312 are binaries and takes in average 3 h to run. This difference occurs because of the DSM Equation (Equation (3) in which $\boldsymbol{a_{it}}$ is an input for Model I, but a decision variable for Model II). This makes Model II considerably larger than Model I.

To reduce the computing times of Model II, a heuristic was implemented. It is based on prescribing a smart starting point for the DSM: harder minerals should be processed during daylight

Table 3
Definition of cases.

Case	Models used	Contracted power MW	PV plant MW	BESS energy capacity, MWh	BESS inverter capacity, MW
BC	I & II	43	20	10	2
C1	I	43	0 – 120	10	2
C2	I & II	39.7–43	20	10	2
C3	I	40.5 & 41.5	20	0.1 – 60	2
C4	I	41, 41.2, 41.5 41.8 & 42	20	10	0 – 3

time (when PV power is available). For this, the SAG demand vector is rearranged as a function of the PV generation curve prior to the optimization as it is seen in Fig. 4. In the night, where PV generation is zero, the remaining power consumption points are allocated first, in a descending order, from 21 to 24 h (after daytime hours), and then, in a descending order, from 0 to 8 h (before daytime hours). This is done using a search and allocate algorithm. This heuristic reduces the processing times by 55–90% (for more details consult the next section). Further time savings could be achieved by running the optimization on a cluster, as this kind of problems offer parallelization options.

3. Results and discussion

The model was run for different cases. The base case (BC) defines the base contribution that can be obtained by using a constant PV and BESS system, considering the investment costs. Case 1 (C1) studies the impact of changing the size of the PV plant. In this case, the DSM is justified by showing different total costs curves, which include operational and investment cost. The contracted power capacity variation in Case 2 (C2) allows seeing the effect of decreasing the contracted power capacity before incurring into consumption above the contracted capacity, showing the point of possible power consumption stabilization. In cases 3 and 4 (C3 & C4), the BESS energy capacity and power variation show what battery size will be needed to manage different power contracts that allow further costs reduction.

3.1. Base case

In the base case, the results for Model I and II are quite similar (Fig. 2). Both achieve a 15.7% operational cost reduction, when compared to the situation without the PV power plant and BESS. Considering the investment costs, a 4.6% cost reduction is achieved. Since the power contract is above the maximum consumption, and there is no PV energy excess to export, the DSM does not play a role here.

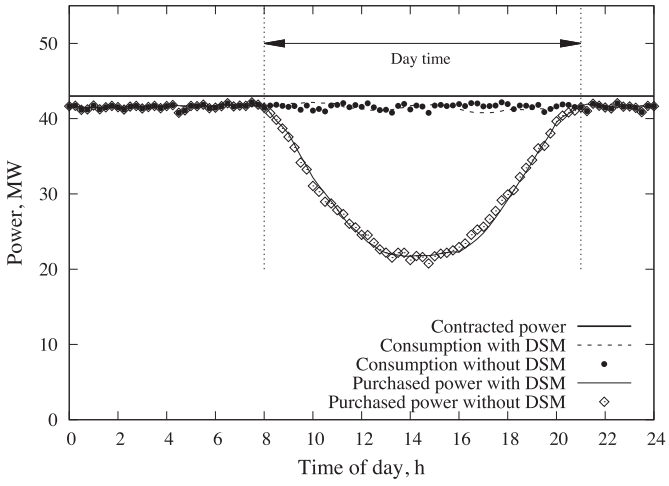

Fig. 2. Purchased power with and without PV plant and BESS.

3.2. Case 1: Impact of PV power plant size

The simulations for C1 show the different behaviors of the system in response to PV plant sizes. Larger PV sizes contribute to operational savings, in the order of 0.78%/MW_{PV}. When considering the investment costs, the savings are 0.22%/MW_{PV}. This means that a 100 MW PV power plant, can achieve 22% of savings. Model I & II give the same results.

As the cycling of the BESS is costly, its usage is limited when the contracted power is higher than the maximum SAG power consumption, which is 42.17 MW. In fact, the imported energy matches demand during the night, the PV plant provides the supplement during the day, and the BESS shows no activity. Also, the DSM at low PV generation does not contribute towards lower costs. There is no value in managing energy if there is no energy excess to be managed.

On the other hand, when the generated PV energy is higher than the maximum consumption during daytime, the system prefers to export the energy rather than managing it with the BESS and incurring into cycling. At this point the total cost curve stops being linear and starts progressively increasing its slope. The change in slope is explained by the difference between selling and purchasing price of energy to and from the grid. Approximately, the total cost saving decreases to 0.20%/MW_{PV}.

The total costs for different load curves (but with the same energy demand) illustrate the effect of allocating the maximum consumption during daytime (Fig. 3). Three different cost curves

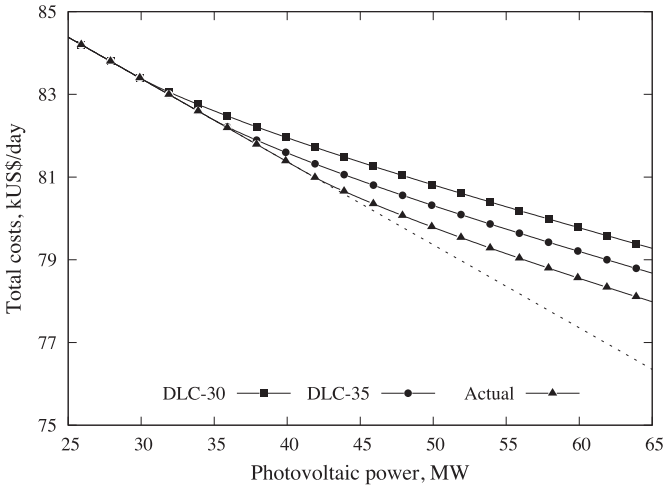

Fig. 3. SAG mill total cost as function of PV energy availability without DSM considering actual maximum consumption (~ 42 MW) and with a daytime maximum consumption of 30 MW and 35 MW.

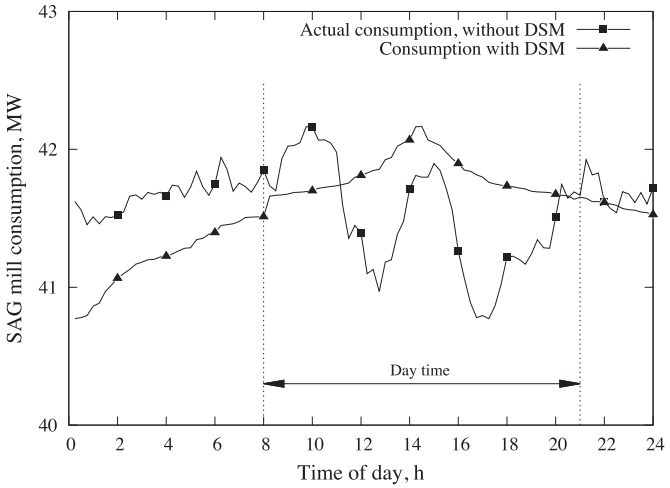

Fig. 4. Operation of SAG mill, with and without DSM.

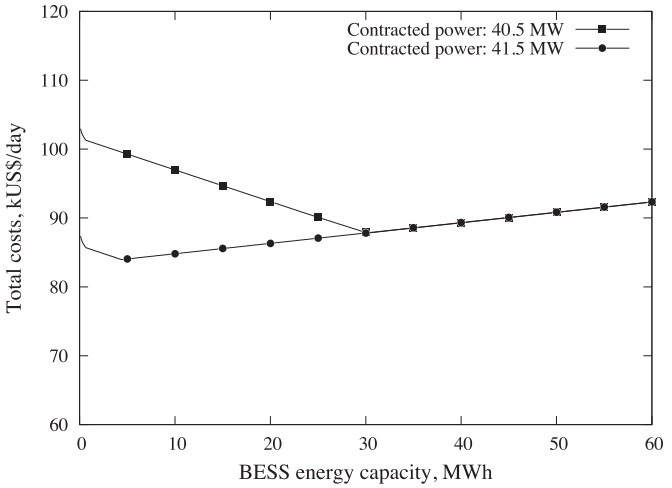

Fig. 6. Total cost against BESS energy capacity variation for different contracted power.

were obtained using: i) the actual SAG mill power load; and assuming a maximum load during daytime of ii) 35 MW, and iii) 30 MW. The dotted line shows the total cost when all the PV energy is used by the SAG mills, and no energy is sold to the grid. As the total cost curve breaks right at the maximum SAG mill power load, the difference between the three curves and the dotted line shows the potential savings of DSM.

3.3. Case 2: Impact of contracted power capacity

Results of C2 show that the DSM has an important role when making a decision on the contracted power capacity. Especially, for lower contracted power capacities, not managing the feed leads to important penalty costs.

For this case, the difference of operation with and without DSM is depicted. It can be observed that a higher power consumption occurs during daytime as seen in Fig. 4.

Fig. 5 shows the minimum power contract, in which no penalty fees due to overconsumption are incurred. When the actual power consumption is considered, the minimum is 41.2 MW. If the ore feed is properly sequenced through DSM, this limit can be lowered by 0.5 MW.

When the contracted power capacity is high, the BESS shows no activity, as in the BC. However, for lower contracted power capacities, the model prefers to use the BESS than incurring into overconsumption fines.

Noteworthy is that the optimized curve generated by the DSM of a contracted power equal or less than 40.7 MW is the optimum consumption curve for every case. The ones generated over this value, are local optima for their value and higher contracted power capacities. A lower contracted power means that the imported energy from the grid can be stabilized to that point complementing the remaining power from the sun, through PV generation. As the PV-BESS parameters are fixed in this case, the constant cost gap occurring on lower contracted power represents the overconsumption penalties.

3.4. Case 3: Impact of BESS energy capacity

C3 analyzes the importance of the BESS energy capacity. As it can be seen in Fig. 6, a minimum cost is achieved, which also depends on the contracted power. For a contracted power of 41.5 MW, the minimum is achieved with a 4.4 MWh BESS energy capacity, while for 40.5 MW contracted power, the minimum with a 30.2 MWh BESS.

To the left of the minimum, the costs increase due to power

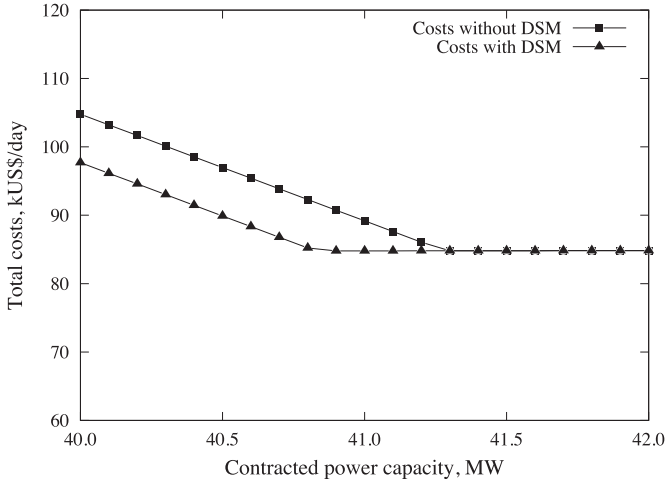

Fig. 5. The total costs corresponding to the contracted power variation.

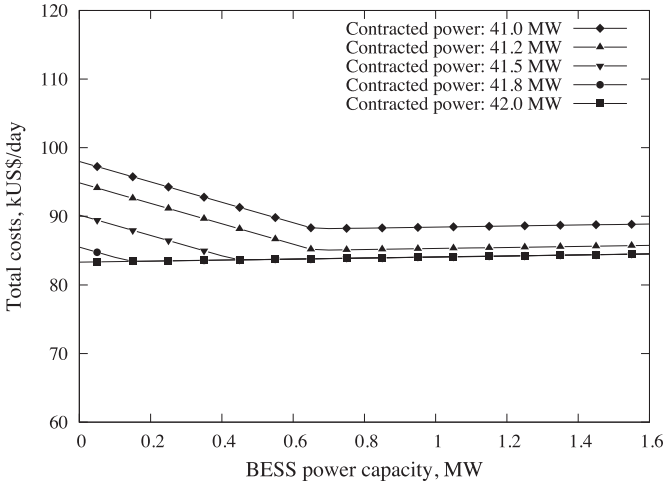

Fig. 7. Total costs against BESS power capacity for different contracted power.

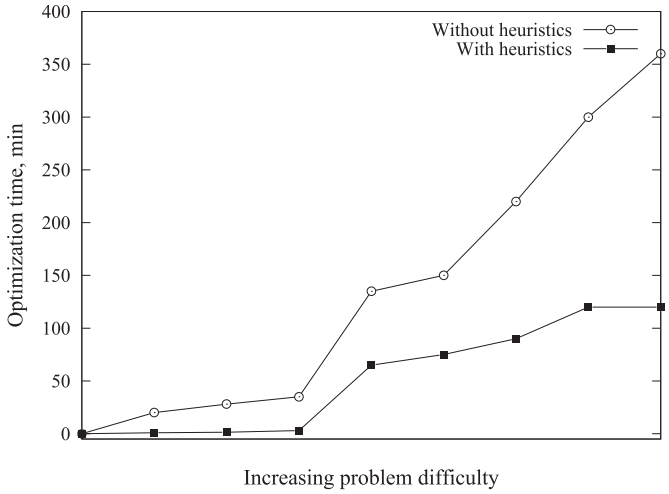

Fig. 8. Solving times of Model II with and without the heuristic, sorted by increasing problem difficulty.

consumption above the contracted capacity. For larger BESS energy capacities, the cost starts raising due to higher investment/replacement costs of the BESS. This shows the optimum BESS needed to manage energy to prevent overconsumption and take account of all other variabilities.

3.5. Case 4: Impact of BESS power capacity

Results for C4 show that increasing the BESS power capacity produces savings that depend on the contracted power, as seen in Fig. 7. The achievable savings show a saturation point, which is reached with a BESS of 0.15, 0.45, 0.70 and 0.70 MW for a contracted power of 41.8, 41.5, 41.2 and 41.0 MW. For 42 MW it can be seen that the costs are almost constant. The cost reduction strongly depends on the contracted power. As expected, a low contracted power has to be compensated with a larger BESS.

There is a maximum effective BESS power capacity size after which no further cost reduction is observed. This value depends on the contracted power. In C4, for contracted powers of 41.2 and 41.0 MW, the maximum effective BESS power is 0.7 MW. On the other hand, if the contracted power is 41.5 MW, a BESS with power capacity of 0.45 MW is enough. In general, an increase of the BESS power capacity allows lowering the contracted power. However, since in C4 the PV plant size is constant, a decrease in the contracted power at some point cannot be overcome by an increase in BESS capacity, and overconsumption may occur because of a deficit in the energy balance. This can be inferred from the cost gap between contracted powers of 41.2 and 41.0 MW, for BESS power higher than 0.7 MW in Fig. 7.

3.6. Impact of demand side management

The DSM has a great impact on how the solar energy can be used and on the investment that has to be made in BESS and the PV system. Although the overall SAG mill energy consumption does not change with DSM, its implementation allows a deeper integration of solar energy into the process. The DSM allocates harder ores (higher energy consumption) during daytime and softer ores during the night, resulting in a smoother net load. This in turn, allows for smaller capacity contracts without incurring into overconsumption fines. For a constant capacity contract and PV plant power capacities, DSM displaces the need for larger BESS (energy and power capacity) implying that lower investments are needed to accomplish better results. The costs related to DSM were not assessed in this study.

DSM also impacts the solving times (Model II requires on average 3 h), which is why a heuristic was developed. Inspired on the above results, where it can be observed that the highest demand is assigned during the day and the lowest during the night (see Fig. 4), the heuristic prescribes a good initial solution. This allows for a drastic reduction (more than 50%) of solving times. Scenarios that are easy to solve take about 90 s, whereas the harder ones take about 90 min. Fig. 8 shows a comparison of solving times for Model II with and without the heuristic.

The results show that problems distant from overconsumption (when the plant or contract are oversized) have short processing times, compared to those where exceeding the contract is at stake.

3.7. Study case results summary

A summary of the main results is presented on Table 4.

4. Conclusions

In this paper, a novel short-term optimization for the joint operation of a semi-autogenous grinding mill, photovoltaic power plant and a battery energy storage system (SAG-PV-BESS) is

Table 4
Results summary.

Case	Variable	Main results
1	PV size	• Cost savings of over 0.2%/MWPV can be achieved in all scenarios. A PV plant of 100 MW can achieve a 20% of savings. • (Contracted power sensitivities are not considered.) • DSM has an important influence on cost reduction potential. • (BESS sensitivities are not considered.)
2	Contracted power and DSM	• (PV size sensitivities are not considered.) • Contracted power can be reduced with DSM from 41.2 to 40.7 MW. • DSM shows a cost reduction potential of about 10%. • BESS has no important role under large power contracts, while it helps avoiding fines under smaller contracts.
3	BESS Energy capacity	• Larger BESS energy capacities do not contribute to further savings due to the limited PV size (of this scenario). • A larger BESS energy capacity allows for smaller power contracts. • (DSM is not considered.) • For a contracted power of 41.5 and 40.5 MW, the resulting energy capacities are 4.4 and 30.2 MWh.
4	BESS power capacity	• Larger BESS power capacities do not contribute to further savings due to the limited PV size (of this scenario). • There is a minimum BESS power capacity needed to avoid fines associated with each power contract. • (DSM was not considered) • For a contracted power of 41.5 MW, the resulting BESS is 0.45 MW.

presented. Further, a demand side management (DSM) option, based on sorting the rocks' hardness, is modeled and assessed. Finally, a heuristic to reduce the solving times of the model (with DSM) was implemented.

The results show that when the contracted power capacity is above SAG maximum load, the BESS plays a minor role. Here, PV excesses are exported to the grid instead of being stored, to avoid the cycling costs of the batteries. The BESS, therefore, will only be used to avoid overconsumption.

For a given contracted power capacity and PV plant size, the simulations allow finding the optimal BESS size. For BESS smaller than that optimum, the cost increases due to overconsumption; and for those larger than the optimum due to higher investment costs of the batteries. Overall, the results show that a PV-BESS system is already an economically attractive solution for copper mining operations in Atacama.

DSM show an additional saving potential of about 10%. If DSM implemented, the system allocates the harder ores when PV energy is available (daytime). Moreover, the implementation of DSM together with the BESS can contribute to safely reducing the contracted power capacity. Finally, the DSM proves to have a great impact on the PV and BESS sizes. By implementing DSM, a larger integration of solar energy into the process can be achieved.

The proposed heuristic (finding a good initial solution for the model with DSM) allows reducing the involved solving times by over 50%. Developing further speed-up techniques are envisioned for solving stochastic frameworks.

Acknowledgments

This work was supported by the Chilean National Commission for Scientific and Technological Research (CONICYT), through the Solar Energy Research Center SERC-Chile (FONDAP 15110019) and the Solar Mining project (CONICYT-BMBF 20140019), and the German Academic Exchange Service (DAAD). This work made use of the free plotting package Gnuplot.

References

Beaudin, M., Zareipour, H., Schellenberglabe, A., Rosehart, W., 2010. Energy storage for mitigating the variability of renewable electricity sources: an updated review. Energy Sustain. Dev. 14 (4), 302–314.

Chung, D., Davidson, C., Fu, R., Ardani, K., Margolis, R., 2015. Us Photovoltaic Prices and Cost Breakdowns: Q1 2015 Benchmarks for Residential, Commercial, and Utility-scale Systems. Tech. rep.. NREL Technical Report.

Cochilco, 2013. Actualización de información sobre el consumo de energía asociado a la minería del cobre al año 2012. Tech. rep.. COCHILCO.

Fuentealba, E., Ferrada, P., Araya, F., Marzo, A., Parrado, C., Portillo, C., 2015. Photovoltaic performance and LCoE comparison at the coastal zone of the Atacama Desert, Chile. Energy Convers. Manag. 95, 181–186.

Haas, J., Cebulla, F., Cao, K., Nowak, W., Palma-Behnke, R., Rahmann, C., Mancarella, P., 2017. Challenges and trends of energy storage expansion planning for flexibility provision in low-carbon power systems—a review. Renew. Sustain. Energy Rev. 80, 603–619.

Hajipour, E., Bozorg, M., Fotuhi-Firuzabad, M., 2015. Stochastic capacity expansion planning of remote microgrids with wind farms and energy storage. IEEE Trans. Sustain. Energy 6 (2), 491–498.

Harmsen, J., Roes, A., Patel, M.K., 2013. The impact of copper scarcity on the efficiency of 2050 global renewable energy scenarios. Energy 50, 62–73.

Levesque, M., Millar, D., Paraszczak, J., 2014. Energy and mining—the home truths. J. Clean. Prod. 84, 233–255.

MATLAB Documentation, 2014. Mixed-integer Linear Programming (MILP) - MATLAB Intlinprog [online] Available at: https://www.mathworks.com/help/optim/ug/intlinprog.html (Accessed 8 June 2017).

McLellan, B., Corder, G., Giurco, D., Ishihara, K., 2012. Renewable energy in the minerals industry: a review of global potential. J. Clean. Prod. 32, 32–44.

Morrell, S., 2004. Predicting the specific energy of autogenous and semi-autogenous mills from small diameter drill core samples. Miner. Eng. 17 (3), 447–451.

Mosher, J., Bigg, A., 2001. SAG mill test methodology for design and optimization. Proc. Int. Autogenous Semiautogenous Grind. Technol. 1, 348–361.

Norgate, T., Haque, N., 2010. Energy and greenhouse gas impacts of mining and mineral processing operations. J. Clean. Prod. 18 (3), 266–274.

Protogeropoulos, C., Brinkworth, B., Marshall, R., 1997. Sizing and techno-economical optimization for hybrid solar photovoltaic/wind power systems with battery storage. Int. J. Energy Res. 21 (6), 465–479.

Schill, W.-P., 2014. Residual load, renewable surplus generation and storage requirements in Germany. Energy Policy 73, 65–79.

Schoenung, S.M., Burns, C., 1996. Utility energy storage applications studies. IEEE Trans. Energy Convers. 11 (3), 658–665.

Steinke, F., Wolfrum, P., Hoffmann, C., 2013. Grid vs. storage in a 100% renewable Europe. Renew. Energy 50, 826–832.

Suazo-Martínez, C., Pereira-Bonvallet, E., Palma-Behnke, R., 2014. A simulation framework for optimal energy storage sizing. Energies 7 (5), 3033–3055.

Suberu, M.Y., Mustafa, M.W., Bashir, N., 2014. Energy storage systems for renewable energy power sector integration and mitigation of intermittency. Renew. Sustain. Energy Rev. 35, 499–514.

US Department of Energy, 2016. DOE Global Energy Storage Database.

Workman, L., Eloranta, J., 2003. The effects of blasting on crushing and grinding efficiency and energy consumption. In: Proc 29th Con Explosives and Blasting Techniques. Int Society of Explosive Engineers, Cleveland OH, pp. 1–5.

Yao, D., Choi, S., Tseng, K., Lie, T., 2009. A statistical approach to the design of a dispatchable wind power-battery energy storage system. IEEE Trans. Energy Convers. 24 (4), 916–925.

Zerrahn, A., Schill, W.-P., 2015. A Greenfield Model to Evaluate Long-run Power Storage Requirements for High Shares of Renewables. DIW Berlin Discussion Paper.